Available online at **www.joac.info**

ISSN: 2278-1862

Journal of Applicable Chemistry

2018, 7 (3): 559-568

(International Peer Reviewed Journal)

Effect of Cadmium Incorporation on Optical and Electrical Properties of Nickel doped Zinc Phosphate Crystals

Delma D'Souza[1], N. Jagannatha[1]*, K.P. Nagaraja[1] and K.B. Reema[1]

1. Post Graduate department of Physics, FMKMC College, Mangalore University, Madikeri-571201, Karnataka, **INDIA**

Email: jagannathnettar@yahoo.co.in

Accepted on 14th April 2018

ABSTRACT

Nickel doped Zinc Phosphate (NZP) and Cadmium incorporated NZP (CNZP) crystals were grown in silica hydro gel media. Specific gravity of Sodium Meta Silicate (SMS), gel setting time, pH of the gel, concentrations of ortho-phosphoric acid and concentration of supernatant solutions were varied to establish the optimum conditions for growth. Energy Dispersive X-ray (EDX) measurements predicted the matrix of Cd^{2+} ions with parental NZP crystal. FTIR spectral studies confirmed the presence of phosphate group, water molecules and metal oxygen link in NZP and CNZP crystals. Thermo Gravimetric Analysis (TGA) showed the thermal stability of the crystals upto 900^0C in their anhydrous state. From UV visible spectrophotometric studies band gap energy measured was 6.09eV for CNZP crystal. Electrical conductivity of NZP crystal is enhanced after incorporation of Cd^{2+} ion to form CNZP crystal.

Graphical Abstract

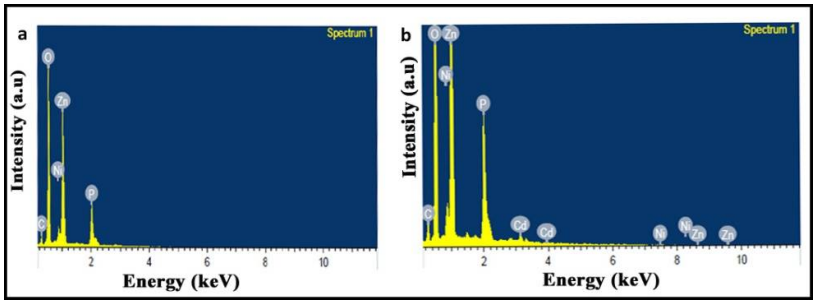

EDX spectrum of (a) NZP and (b) CNZP crystals

Keywords: Doping, Silica hydro gel, Nickel doped Zinc Phosphate (NZP), Cadmium incorporated NZP (CNZP).

INTRODUCTION

Crystals exist in most ordered form and are appropriate in understanding physical and chemical properties of solids [1]. Crystals like GaAs, CdS and InSb exhibit semiconducting behavior and they

are used in developing electronic devices, solar cells and energy storage devices [2]. Certain crystals (Rochelle salt, quartz and tourmaline) show piezo-electricity. These are also used in developing sonar, ultrasound transducers, computer chips and digital watches [3]. Inorganic phosphate crystals have drawn the attention due to the flexibility of PO_4 group as they support the formation of variety of structures [4]. Zinc Phosphate shows adhesion property and finds its application in cementation of inlays, crowns, bridges and orthodontic appliances [5]. Zinc Phosphate crystals are also used as etch resist materials due to their excellent corrosion resistivity [6]. Manganese doped Zinc Phosphate crystals exhibit luminoscence and used as phosphors in cathode ray tubes [7]. Although Zinc Phosphate crystals associated with variety of applications, not many systematic studies were carried out. We report in this paper studies on zinc phosphate crystals aimed at growing nicked doped zinc phosphate (NZP) crystals and Cadmium induced Nickel doped Zinc Phosphate (CNZP) crystals. These crystals were characterized and effect of Cd^{2+} incorporation on optical and electrical properties of NZP crystals was studied.

MATERIALS AND METHODS

Chemicals used for growing NZP and CNZP crystals are SMS ($Na_2SiO_3.9H_2O$), ortho-phosphoric acid (H_3PO_4), zinc Chloride ($ZnCl_2$) and nickel chloride ($NiCl_2.4H_2O$) and cadmium chloride ($CdCl_2.2.5H_2O$) of AR grade.

Single test tube gel diffusion method is employed to grow NZP and CNZP crystals at room temperature. Silica hydro gel provides the growth media and it is prepared by adding 1N ortho-phosphoric acid to SMS solution drop by drop with constant stirring in different ratios. SMS solutions of specific gravities 1.04 to 1.07g cm^{3-1} are prepared by diluting stock solution [8-10]. Ortho-phosphoric acid behaves as acidifying agent and provides the anions needed for crystallization of the compound. The resulting solution is transferred to test tubes and allowed to set for gelling. For NZP, crystal the mixture of supernatant solutions of zinc chloride and nickel chloride added to the set gel and for CNZP, supernatant solutions of zinc chloride, nickel chloride and cadmium chloride are added. Slow inter diffusion of feed solution in gel results in the growth of crystals [11]. In order to establish the optimum growth conditions, experiments were conducted by varying concentrations of orthophosphoric acid, concentrations of supernatant solution and ratios of supernatant mixture in different trials. The chemical reactions describing the formation of NZP and CNZP crystals are,

$$3Ni^{+2} + 3ZnCl_2 + 4H_3PO_4 \rightarrow (Ni: Zn)_3(PO_4)_2.4H_2O + 2POCl_3 + 2H_2O.$$

$$3Cd^{+2} + 3Ni^{+2} + 3ZnCl_2 + 4H_3PO_4 \rightarrow (Cd: Ni: Zn)_3(PO_4)_2.4H_2O + 2POCl_3 + 2H_2O.$$

established optimumconditions for the growth of NZP and CNZP are tabulated in table 1. Harvested NZP and CNZP crystals are shown in figure 1.

Table 1. Optimum conditions for growth.

Crystal	Sp. Gravity of SMS	SMS to H_3PO_4 ratio	pH of the gel	Gel setting time	Gel aging	Cd^{+2} : Ni^{+2}: Zn^{+2}	Color
NZP	1.05	5: 5	6	24 h	8 h	0 : 2 : 5	Yellowish green
CNZP	1.06	5:6	6.4	30 h	6 h	2 : 2: 5	Yellowish green

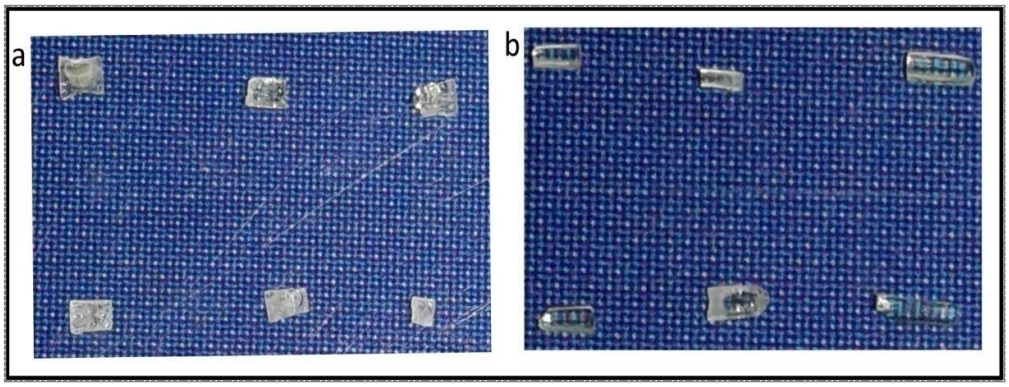

Figure 1. Harvested NZP (a) and CNZP(b) crystals

Characterization: Elemental composition of the grown crystals was determined using CARL ZIESS FESEM attached with EDS system (Oxford instruments). EDX analysis is used for chemical characterization of materials to detect chemical elements present in nanometers depth from the surface of crystal [**12, 13**]. Functional groups of crystals are identified using Bruker (Alpha). FTIR analysis (using FTIR spectrophotometer within the wave number range 400-4500 cm^{-1}) is the spectroscopic technique used for analyzing the structural units of samples from their vibrational modes [**14, 15**]. Thermal properties of NZP and CNZP crystals are studied by TGA using DSC-TGA TA (SDT-Q600) instrument. TGA finds the percentage weight loss of a sample for the increase in temperature [**16, 17**]. Powder XRD studies of the crystals are carried out with the aid of powder XRD analyzing instrument Minflex 600 Rigaku having X-ray Cu-K alpha of wavelength 1.54 A0 at a scan speed of 10 min^{-1}. Optical absorption studies are carried out using UV-Visible Spectrophotometer (UV-1800 SCHIMADZU) in the spectral range 190-1000 nm. Electrical conductivities of the crystals are measured using Roy instruments (IR-503, Sl. No.CDM-17076) operating in the range of 0-1000 mMho cm^{-1}.

RESULTS AND DISCUSSION

EDX spectra of NZP and CNZP are shown in figure 2. The peaks present in the spectrum infer the presence of zinc, nickel, oxygen and phosphorous in NZP crystal and an additional peak in CNZP crystal represent incorporated cadmium. The atomic and weight percentages of detected elements in NZP and CNZP are recorded in table 2. The FESEM images (Fig. 3) with a resolution 100x at 100 µm range identified the valley regions and crystal deformations associated with the crystals.

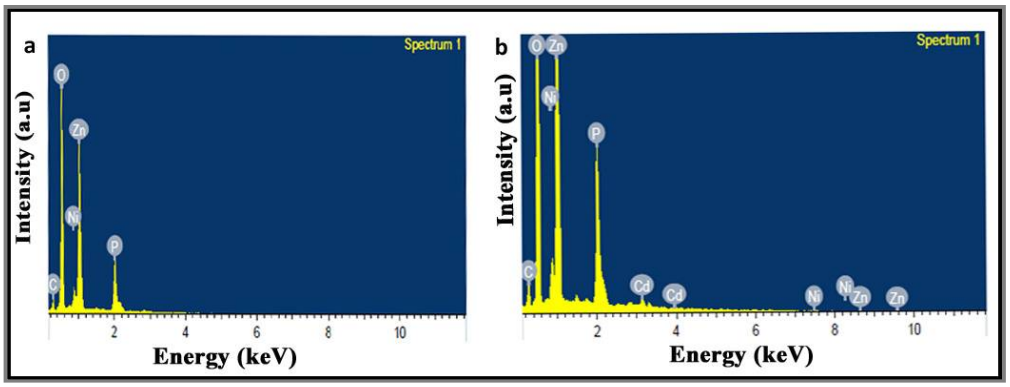

Figure 2. EDX spectrum of (a) NZP and (b) CNZP crystals.

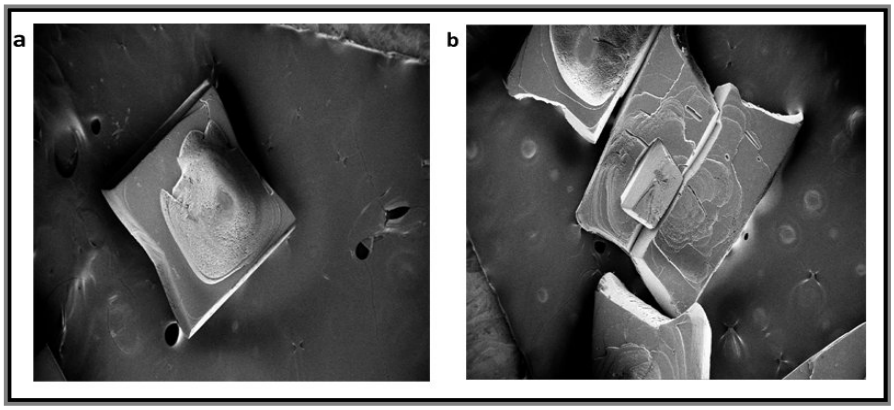

Figure 3. FESEM image of (a) NZP and (b) CNZP crystals.

Table 2. Atomic and weight percentages of constituents of NZP and CNZP crystals.

Crystal	Elements	Atomic %	Weight %
NZP	Zn	15.988	39.893
	P	08.777	10.554
	O	73.043	44.658
	Ni	02.192	04.895
CNZP	Zn	15.981	38.764
	P	11.195	12.805
	O	70.325	41.625
	Ni	01.770	03.846
	Cd	00.729	02.960

FTIR spectra (Fig. 4) shows the shift in absorption peaks of NZP crystals after doped with Cd^{2+} ion to form CNZP crystal. Table 3 shows the band assignments of vibrational modes associated with FTIR spectra of NZP and CNZP crystals. Spectra rectified the existence of water of crystallization, phosphate group and metal oxygen (M-O) bonds. Both the crystals showed absorption peaks in the range 3774 cm^{-1} to 3153 cm^{-1} representing symmetric, asymmetric O-H stretching, due to the presence

Table 3. Band assignments in FTIR spectra of NZP and CNZP crystals.

Wave number (cm^{-1})		Band assignments
NZP	CNZP	
3774 3540 3153	3762 3270	Symmetric and asymmetric O-H stretching (water of crystallization)
1602	1601	Internal H-O-H bending
1401	1401	P=O stretching
1106 1022	1109 1025	Asymmetric P-O stretching
948	946	Symmetric P-O stretching
635 578	635 572	Asymmetric O-P-O bending
246 414	427	Symmetric O-P-O bending
454	447	M-O stretching

of water molecules [18]. The absorption band around 1601cm^{-1} corresponds to internal H-O-H bending. The absorption at 1401cm^{-1} indicates P=O stretching. Further, absorption band between 1100

cm^{-1} to 1025 cm^{-1} and at around 948 cm^{-1} represent asymmetric and symmetric P-O stretching in order. The vibrations in the range 635 cm^{-1} to 570 cm^{-1} correspond to asymmetric O-P-O bending. Absorption around 410-430 cm^{-1} is due to symmetric O-P-O bending and O-M stretching [16].

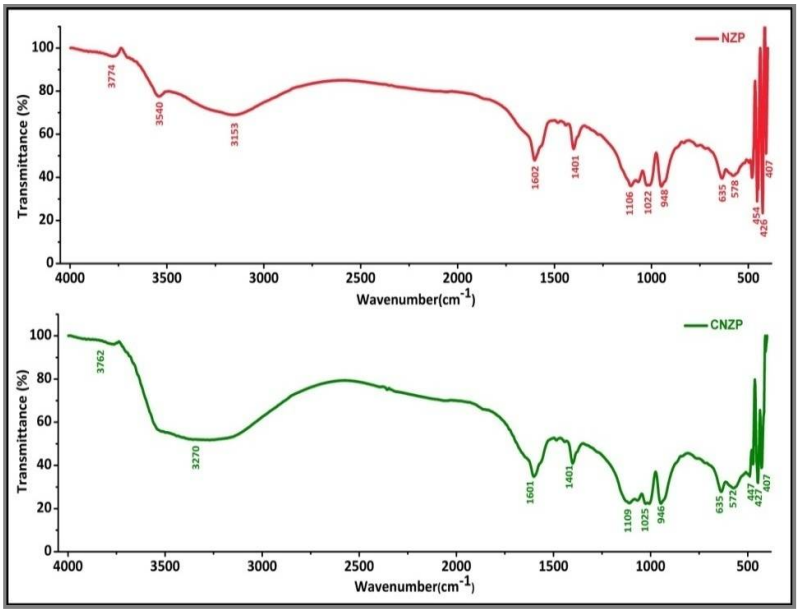

Figure 4. FTIR spectra of NZP and CNZP crystals.

The thermal stability and decomposition phases of NZP and CNZP crystals are analyzed using TG analysis (Figure 5). The curve shows decomposition in two steps losing four water molecules in the crystals. For NZP crystal, the first phase of decomposition occurs between the temperature range 70^0C to 314^0C with a loss of three water molecules to form a monohydrate crystal showing observed weight loss of 12.18% (Calculated loss: 11.797%). The second phase of decomposition occurs in the temperature limit 314^0C-414^0C with observed weight loss of 3.50% (Calculated loss: 3.932%) losing remaining one water molecule forming anhydrous NZP crystal. However in CNZP crystal the first phase of decomposition takes place in the temperature range 66^0C -310^0C showing observed weight loss 11.756% (Calculated loss: 11.797%) and in the second decomposition phase (310-382^0C) the weight loss found to be (observed) 3.82% (Calculated loss: 3.932%) to form anhydrous CNZP crystal. Above 450^0C both the crystals exhibit stability upto 900^0C (not shown in the figure) due to the presence of transition metal ions (Cd^{+2}, Ni^{+2} and Zn^{+2} associated with high melting points) [20]. TG analysis of the crystals depicts that occupation of Cd^{2+} ion in NZP decrease the binding strength of water molecules with lattice, since CNZP crystal decomposes at lower temperature.

Table 4. Phases of decomposition with observed and calculated weight loss.

Crystal	Decomposed Temp (^{0}C)	Process	Weight Loss (%)	
			Observed	Calculated
NZP	70-314	$(Ni:Zn)_3PO_4.4H_2O \rightarrow (Ni:Zn)_3PO_4.H_2O + 3H_2O$	12.180	11.797
	314-414	$(Ni:Zn)_3PO_4.H_2O \rightarrow (Ni:Zn)_3PO_4 + H_2O$	03.500	03.932
CNZP	66-310	$(Cd:Ni:Zn)_3PO_4.4H_2O \rightarrow (Cd:Ni:Zn)_3PO_4.H_2O + 3H_2O$	11.756	11.797
	310-382	$(Cd:Ni:Zn)_3PO_4.H_2O \rightarrow (Cd:Ni:Zn)_3PO_4 + H_2O$	03.820	03.932

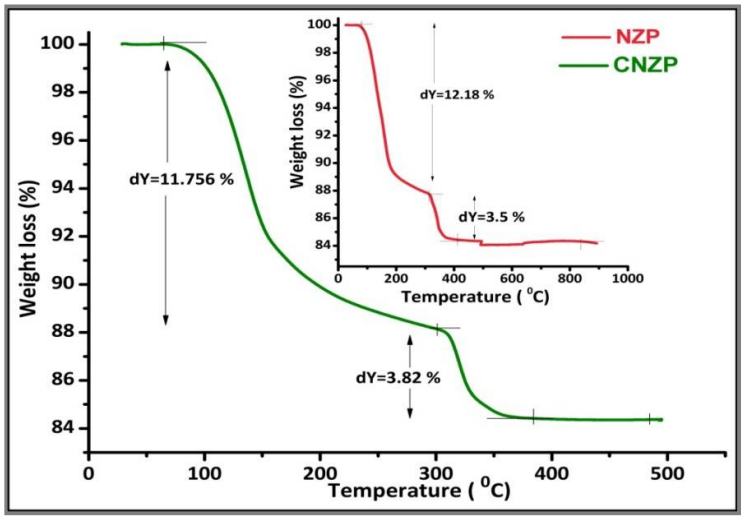

Figure 5. TGA plot of NZP and CNZP crystals.

Powder XRD patterns (Figs. 6, 7) show high crystallinity nature of NZP and CNZP crystals. N-TREOR09 program was used to index the crystals P-XRD data and the plot showed sharp well defined peaks for specific 2θ values [**19**]. Both the crystals belong to orthorhombic system with space groups *Pmna* (for NZP) and *Pbnm* (for CNZP) are recorded in Table 5. Results obtained are in agreement with the standard values of JCPDS data reported [**20**].

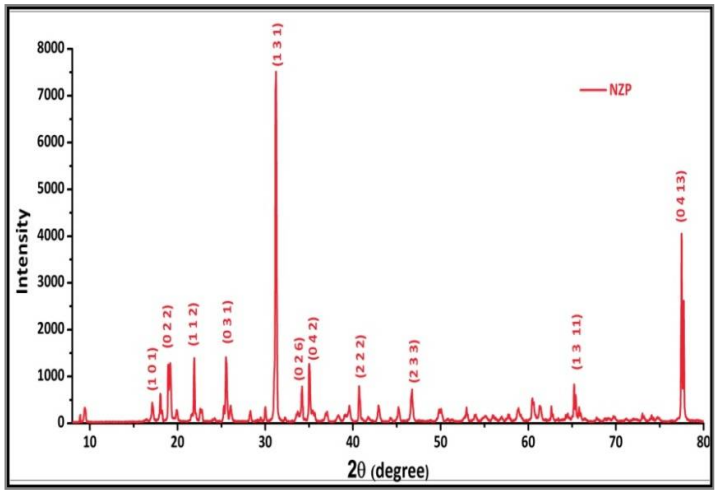

Figure 6. Powder XRD pattern of NZP crystal

Table 5. Lattice parameters of NZP and CNZP crystals.

Lattice parameters	NZP	CNZP
a (A^0)	5.0423	5.0247
b (A^0)	10.6895	10.6480
c (A^0)	18.0291	18.0575
α (^{0})	90	90
β (^{0})	90	90
γ (^{0})	90	90
Space group	Pmna	Pbnm
Crystal system	Orthorhombic	Orthorhombic

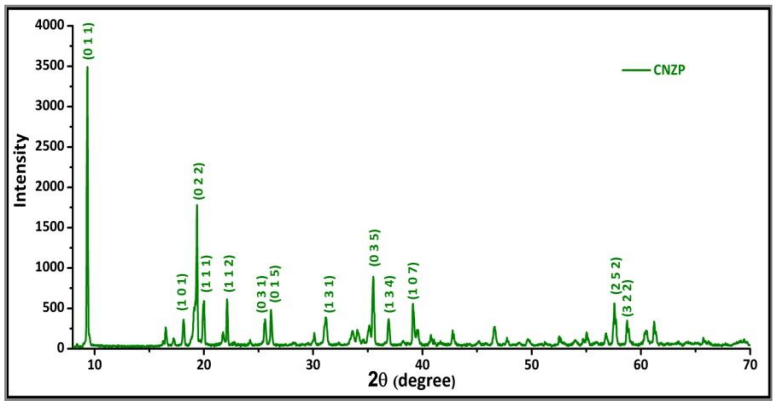

Figure 7. Powder XRD pattern of CNZP crystal

Optical studies (using UV visible spectroscopy) of parental NZP and doped CNZP crystals were carried out for the wavelength range 190nm to 1000nm of the incident photons. UV visible absorption and transmittance spectra NZP and CNZP crystals are displayed in figure 8. NZP crystal shows absorption in the range 190nm-270nm (correspond to UV region) with absorption maximum (A_{max}) of 0.079. However, CNZP crystal can absorb light in the wider range from 190nm-400nm with A_{max} 0.301.

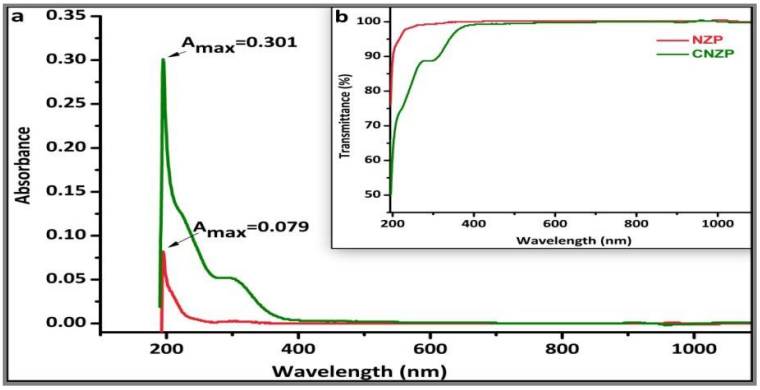

Figure 8. UV visible (a) absorption and (b) transmittance spectra of NZP and CNZP crystals

Further, for the entire visible region both the crystal shows maximum transparency. The spectra is regenerated as Tauc plot to find the energy gap (Figure 9). Band gap energies of NZP and CNZP crystals are 6.15eV and 6.09eV respectively. This elucidates the insulating behaviour of crystals [21]. The difference in band gaps of the crystals suggests that two crystals are distinct. Thus reinforcement of Cd^{2+} ion with parental NZP crystal resulted in the growth of entirely new crystal (CNZP). This enumerates the success in growth and studies of CNZP crystal. One can expect more electrical conductivity in CNZP crystal due to smaller energy gap.

Table 6. Electrical conductivities of NZP and CNZP crystals

Crystal	Electrical conductivity mʊ cm^{-1}	
	27^0C	40^0C
NZP	0.8	0.5
CNZP	5.2	3.7

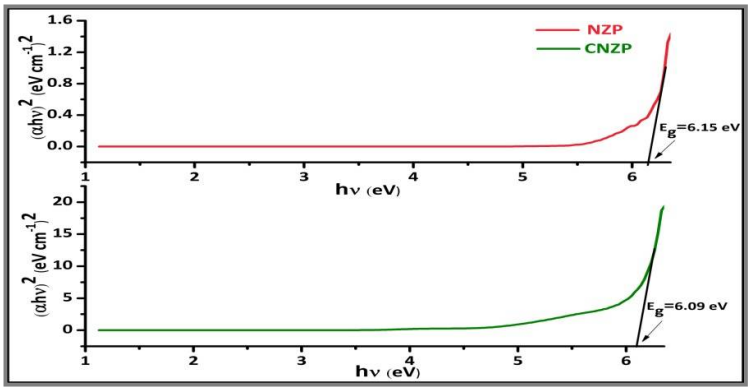

Figure 9. Tauc plots of NZP and CNZP crystals.

Electrical conductivity measurements of crystals were carried out by dissolving the crystals in suitable solvents. 5mg of NZP and CNZP crystals were dissolved in H_2SO_4 (1.5N) and calibrated to measure electrical conductivity [19]. Measurements were carried out at 27^0C (room temperature) and at 40^0C. The results obtained were recorded in Table 6. Conductivity of parental crystal (NZP) was enormously increased due to Cd^{2+} influence. Conductivity measurements predicted that both the crystals are suitable dielectrics at ambient temperature.

The present studies on the grown crystals revealed that doping of Cd^{2+} ion with parental NZP crystal resulted in growth of entirely new crystal (CNZP). EDX measurements, TG analysis and FTIR studies confirmed the incorporation of Cd^{2+} ion, four water molecules and Phosphate group as constituents of CNZP crystal. UV visible studies of the parent and doped crystal identified the insulating behaviour. CNZP crystal possessed more electrical conductivity than parental NZP crystal due to smaller energy gap.

APPLICATION

NZP and CNZP crystals are transparent to visible light. This allows them to be used for window applications where the crystalline perfection and optical transparency is essential. As crystals behave as insulators, they can be used to develop copper clad laminates in PCBs.

CONCLUSIONS

NZP and CNZP single crystals are successfully grown in silica hydro gel media. Optimum conditions established for growth of NZP and CNZP crystals are different. EDX measurements confirmed the existence of Cd^{2+} ion in CNZP crystal. FTIR analysis detects PO_4 units, water of crystallization and the metal oxygen bond associated with the crystals. TG analysis of the crystals shows that occupation of Cd^{2+} ion in NZP decrease the binding strength of water molecules with lattice. PXRD studies infer that both materials crystallize into orthorhombic systems. UV visible and electrical conductivity measurements deduce that incorporation of Cd^{2+} ion in NZP increased the electrical conductivity of CNZP crystal as a result of smaller band gap energy.

ACKNOWLEDGEMENTS

The authors thank UGC New Delhi for financial support under the MANF scheme. We are grateful to scientific officer, DST-PURSE laboratory, Mangalore University, Mangalore for providing laboratory facilities.

REFERENCES

[1]. A. Saranraj, S. S. J. Dhas, M. Jose, S. A. M. B. Dhas, Growth of bulk single crystals of Urea for photonic applications, *Electron. Mater. Lett.*, **2018**, 14(1), 7-13.

[2]. Ruren Xu, Yan Xu, Modern Inorganic Synthetic Chemistry, Jilin University, Changchun, China **2017**.

[3]. I. S. Prameela Kumari, Studies on cadmium based metal organic crystals, Manonmaniam Sundaranar University, Tamilnadu, India, **2011.**

[4]. D. Y. Pan, D. R. Yuan, H. Q. Sun, S. Y. Guo, X. Q. Wang, X. L. Duan, C. N. Luan, Z. F. Li, Solubility and crystallization of $BaHPO_4$ crystals, *Cryst. Res. Tech.*, **2006,** 41, 236-238.

[5]. H. Nariai, S. Shibamoto, H. Maki, I. Motooka, Mechanochemical effects on the reactivity of $Ni_3(PO_4)_2$-$(NH_4)_2HPO_4$-M_2CO_3 (M: Alkaline metal) mixture**,** *Phosphorous. Res. Bull.***, 1998,** 8, 101-106.

[6]. Xiao-Bo Chen, Xian Zhou, Trevor B. Abbott, Mark A. Easton, Nick Birbilis, Double-layered manganese phosphate conversion coating on magnesium alloy AZ91D: Insights into coating formation, growth and corrosion resistance, *Surface Coating. Tech.*, **2013**, 217, 147-155.

[7]. N. Rezaee, M. M. Attar, B. R. Amezanzadeh, Studying corrosion performance, microstructure and adhesion properties of a room temperature zinc phosphate conversion coating containing Mn^{2+} on mild steel, *Surface Coating. Tech.*, **2013**, 236, 361-367.

[8]. N. Jagannatha, P. Mohan Rao, Studies on impurity incorporation in cadmium oxalate crystals grown by gel method, *Bull. Mater, Sci.*, **1993**, 16, 365-370.

[9]. V. Mathivanan, M. Harish, Structural, compositional, optical, thermal and magnetic analysis of undoped, copper and iron doped potassium hydrogen tartrate crystals, *Indian J. of Pure and Applied Phys.*, **2013**, 51, 851-859.

[10]. H. K. Henisch, Crystal growth in gels, The Pennyslvania State Univ. Press, USA, **1970**.

[11]. **S**. M. Dharmaprakash, P. Mohan Rao, Periodic crystallization of barium oxalate in silica hydrogel, *Bull. Mater. Sci.*, **1986, 8, 511-517**

[12]. C. K. Chauhan, P. M. Vyas, M.J. Joshi, Growth and characterization of Struvite-K crystals, *Cryst. Res. Technol.*, **2011**, 46, 187-194.

[13]. T. P. Jyothi, H. R. Manjunath, M. K. Ravindra, M. K. Shivanand, K. M. Mahadevan, N. K. Lokanath, S. Naveen, Synthesis, Characterization and Crystal Structure Analysis of 2-(1-(4-butylphenyl)-4,5- diphenyl-1H-imidazol-2-yl)-4-chlorophenol, *J. Applicable Chem.*, **2018**, 7 (1), 224-233.

[14]. N. Latha Rani, Shivaprasad Shetty, N.V. Anil Kumar, M.A. Sridhar, Synthesis, Spectral Study and Crystal Structure Analysis of Two Coumarin Derivatives, *J. Applicable. Chem.*, **2018**, 7(1), 59-70.

[15]. Khaled M. Mohammad, Ibtisam K. Jasim, Abdullah H. Kshash, Synthesis, characterization and liquid crystals properties for N, N'- (3,3'-dimethylbiphenyl-4,4'-diyl) dialkaneamide, *J. Applicable Chem.*, **2014**, 3(3), 1036-1041.

[16]. C. Justin Raj, G. Mangalam, S. Mary Navis Priya, J. Mary Linet, C. Vesta, S. Dinakaran, B. Milton Boaz, S. Jerome Das, Growth and characterization of non-linear optical zinc hydrogen phosphate single crystal grown in silica gel, *Cryst. Res. Techno.*, **2007**, 42(4), 344-348.

[17]. J. Pramod Patil, Kamlesh D Prajapati, Synthesis and thermal studies of polyesters derived from 6-(N-(3-Chlorophenyl)piperazinyl)-2,4-bis(7-hydroxycoumarin-4-acetylchloride)-1, 3, 5-triazine, *J. Applicable Chem.*, **2017**, 6 (6), 1048-1057.

[18]. P.N.V.V.L. Prameela Rani, J. Sai Chandra, V.Parvathi, Y.Sunandamma, Synthesis and Spectroscopic Investigations of Cu (II) doped Ni L-Histidine Hydrochloride Monohydrate Crystals, *J. Applicable. Chem.*, **2013**, 2(2), 343-351.

[19]. Nagaraja Ponnappa, Jagannatha Nettar, Hema Mylnahalli, Delma D'Souza, Lokanath Neratur, Growth, Characterization and Conductivity of Chromium Mixed Cadmium Oxalate Crystals, *Cryst. Res. Technol.*, **2018**, 53(2), 1700261.
[20]. Laurent Herschke, Volker Enkelmann, Ingo Lieberwirth, Gerhard Wegner, The role of hydrogen bonding in the crystal structures of zinc phosphate hydrates, *Chem. Eur. J.*, **2004**, 10, 2795-2803.
[21]. P. Anandan, G. Parthipan, T. Saravanan, R. Mohan Kumar, G. Bhagavannarayana, R. Jayavel, Crystal growth, structural and optical characterization of a semi-organic single crystal for frequency conversion applications, *Physica B*, **2010**, 405, 4951-4956.